AFRL-RD-PS
TP-2010-1005 Part 2 of 2

INVESTIGATION OF CLOSED LOOP ADAPTIVE OPTICS WITH THE DEFORMABLE MIRROR NOT IN PUPIL - PART 2: THEORY (POSTPRINT)

Darryl J. Sanchez, et. al

Air Force Research Laboratory
3500 Aberdeen Ave SE
Kirtland AFB, NM 87117

1 July 2008

Technical Paper

AIR FORCE RESEARCH LABORATORY
Directed Energy Directorate
3550 Aberdeen Ave SE
AIR FORCE MATERIEL COMMAND
KIRTLAND AIR FORCE BASE, NM 87117-5776

REPORT DOCUMENTATION PAGE

Form Approved
OMB No. 0704-0188

1. REPORT DATE *(DD-MM-YYYY)*	2. REPORT TYPE	3. DATES COVERED *(From - To)*
01-07-2008	Technical Paper	July 1, 2008- October 1, 2008

4. TITLE AND SUBTITLE

Investigation of Closed Loop Adaptive Optics with the Deformable Mirror not in Pupil- Part 2: Theory (Postprint)

5a. CONTRACT NUMBER
In House DF702151

5b. GRANT NUMBER

5c. PROGRAM ELEMENT NUMBER
62890F

6. AUTHOR(S)

Darryl J Sanchez, Katherine Lilevjen, *Troy Rhoadarmer, Mala Mateen, *Denis Oesh, Charles Beckner, *Deborah Fung,
Patrick Kelly, R. Anthony Vincent,
**Roger Petty, **Loretta Arguello

5d. PROJECT NUMBER
2301

5e. TASK NUMBER
SJ

5f. WORK UNIT NUMBER
41

7. PERFORMING ORGANIZATION NAME(S) AND ADDRESS(ES)

Air Force Research Laboratory
3550 Aberdeen Ave SE
Kirtland AFB, NM 87117

*Science Applications Int.
2109 AirPark RD
SE Albuquerque, NM 87106

**Boeing LTS
PO Box 5670
Kirtland AFB NM,87117

8. PERFORMING ORGANIZATION REPORT NUMBER

9. SPONSORING / MONITORING AGENCY NAME(S) AND ADDRESS(ES)

Air Force Research Laboratory
3550 Aberdeen Ave SE
Kirtland AFB NM 87117-5776

10. SPONSOR/MONITOR'S ACRONYM(S)
AFRL/RDSA

11. SPONSOR/MONITOR'S REPORT NUMBER(S)
AFRL-RD-PS-TP-2010-1005 Part 2 of 2

12. DISTRIBUTION / AVAILABILITY STATEMENT

Approved for public release

13. SUPPLEMENTARY NOTES
Accepted for publication at the SPIE annual conference; San Diego, CA; August 2008. 377ABW-2008-0296 26 November 2008. "Government Purpose Rights"

14. ABSTRACT
This is the second of two papers discussing aspects of placing the deformable mirror in a location not conjugate to the pupil plane telescope. The Starfire Optical Range, Air Force Research Laboratory is in the process of developing a high efficiency adaptive optics (AO) system for its 3.5m telescope. The objective is to achieve maximum optical throughput while maintaining diffraction limited performance. This can be achieved by minimizing the number of optical elements which then implies placing the AO system on gimbal. Doing so forces the deformable mirror (DM) to not be conjugate to the pupil. However, placing the DM so that it is not conjugate to the pupil results in degradation in Strehl. Wave optics simulation has shown a 7-15% degradation in Strehl. In the previous paper, we experimentally measured this degradation. Then we determine a means to mitigate this degradation in a manner that is implementable on conventional AO systems. Simulation results are presented to validate the veracity of the mitigation technique.

15. SUBJECT TERMS
Adaptive optics; High Efficiency AO

16. SECURITY CLASSIFICATION OF:			17. LIMITATION OF ABSTRACT	18. NUMBER OF PAGES	19a. NAME OF RESPONSIBLE PERSON
					Pat Kelly
a. REPORT	b. ABSTRACT	c. THIS PAGE			19b. TELEPHONE NUMBER *(include area code)*
Unclassified	Unclassified	Unclassified	SAR	18	505- 846-2094

Standard Form 298 (Rev. 8-98)
Prescribed by ANSI Std. 239.18

Investigation of Closed Loop Adaptive Optics with the Deformable Mirror not in Pupil - Part 2: Theory

Darryl J. Sanchez[a], Katherine Lilevjen[a], Troy Rhoadarmer[b], Mala Mateen[a], Denis Oesch[c], Charles Beckner[a], Deborah Fung[b], Patrick Kelly[a], R. Anthony Vincent[a], Roger Petty[d], Loretta Arguello[d]

[a]Air Force Research Laboratory, Directed Energy Directorate, 3550 Aberdeen Ave SE, Kirtland AFB, NM
[b]SAIC, Lasers & Imaging Technology Lab, 1833 Sunset Place, Suite A Longmont, CO 80501
[c]SAIC, 2109 Air Park Rd. S.E. Albuquerque, NM 87106
[d]Boeing-LTS, PO Box 5670, Kirtland AFB NM

ABSTRACT

This is the second of two papers discussing aspects of placing the deformable mirror in a location not conjugate to the pupil plane of a telescope. The Starfire Optical Range, Air Force Research Laboratory is in the process of developing a high efficiency adaptive optic (AO) system for its 3.5m telescope. The objective is to achieve maximum optical throughput while maintaining diffraction limited performance. This can be acheived by minimizing the number of optical elements which then implies placing the AO system on gimbal. Doing so forces the deformable mirror (DM) to not be conjugate to the pupil. However, placing the DM so that it is not conjugate to the pupil results in a degradation in Strehl. Wave optics simulation has shown a 7-15% degradation in Strehl. In the previous paper, we experimentally measured this degradation. In this paper, we determine the cause of the degradation. Then we determine a means to mitigate this degradation in a manner that is implementable on conventional AO sytems. Simulation results are presented to validate the veracity of the mitigation technique.

Keywords: Adaptive Optics, High Efficiency AO

1. INTRODUCTION

Many astronomical observatories are designing their AO systems with the deformable mirror not conjugate to the pupil. This is done for a variety of different reasons ranging from the need to perform multi-conjugate adaptive optics (MCAO) to the need to minimize the number of optical surfaces in order to improve throughput. An innovative approach used by some telescopes converts the secondary mirror into a deformable mirror (DM). At wavelengths longer than $2\mu m$ where there is a need to limit the number of warm surfaces, an optical design with an adaptive secondary minimizes surfaces thereby maximizing sensitivity making it particularly suitable for thermal infrared astronomy. For infrared astronomy an adaptive secondary is also attractive for MCAO since the secondary is roughly conjugate to the strong ground layer.[1,2]

The $6.5m$ Multiple Mirror Telescope (MMT) at Mt. Hopkins in Southern Arizona is the first in the world to use an adaptive secondary[3,4] for wavefront sensor correction. Placing the DM at secondary in this case allows for higher throughput, lower emissivity, and a simpler optical setup. Miller et al.[4] report the measured Strehl to be 40 % of the diffraction limited peak.

The Large Binocular Telescope (LBT) on Mt. Graham, Arizona has two $8.4m$ primary mirrors and two $0.91m$ Gregorian secondary mirrors. The secondary mirrors are the deformable mirrors for the LBT adaptive optics system.[1] The DMs for the LBT were designed based on the successful MMT adaptive secondary design. The Very Large Telescope (VLT) at Paranal, Chile will upgrade one of the $8m$ telescopes to include a deformable secondary mirror (DSM).[5]

The Starfire Optical Range (SOR) is also developing a high-efficiency AO system for its $3.5m$ telescope. One proposed configuration replaces the turning flat M4 with the DM. In this geometry, the DM is $1Km$ (in output space) behind the $3.5m$ primary mirror. Waveoptic simulation of this geometry by Foucault[6] indicated that this geometry leads to a 7-15% degradation in Strehl.

This research seeks to replicate this degradation experimentally, i.e verify that the degradation is not a simulation anomaly, to find the root cause of the degradation, and then to determine if a means to mitigate the degradation was possible. As such, our research consisted of two parts, experimental and theoretical. Experimentally, we built an AO testbed of the proposed DM-not-in-pupil (DNiP) geometry[7] and conducted a set of experimental tests. This experiment verified the existance of the degradation and we measured a 7-9% degradation in Strehl. These results are presented in Part 1 of this two part series.

In this paper, we discuss the root cause of the degradation and also present a means to mitigate the degradation in such a way that it is implementable on conventional AO systems. To this end, Section 2 details SOR's DM-Not-in-Pupil (DNiP) geometry under which the problem arises. Section 3 determines the root cuase of the degradation. Section 4 calculates a closed form algebraic solution. Section 5 proposes a theoretical description for the DNiP degradation. Section 6 presents a mitigation techniuqe, and Section 7 concludes our findings on closed loop Strehl performance with DNiP.

2. BACKGROUND

A conventional AO system places the DM conjugate to the pupil. Doing so causes rays at the DM, aside from magnification, to have the same height and angle as rays at the pupil. In this configuration, the science and beacon beams at both the pupil and DM have the same geometry. So when the DM uses the beacon beam measured at the DM-plane to correct the science beam in the DM-plane, the AO correction is always proper. Placing the DM so that it is not conjugate to the pupil does not necessarily cause the correction to be in error; for instance when natural guidestar AO is used *and* the pupil-DM separation's Fresnel number is high, the correction will be proper.

However, the geometry shown in Figure 1 does induce a degradation in Strehl. In this geometry, (1) the

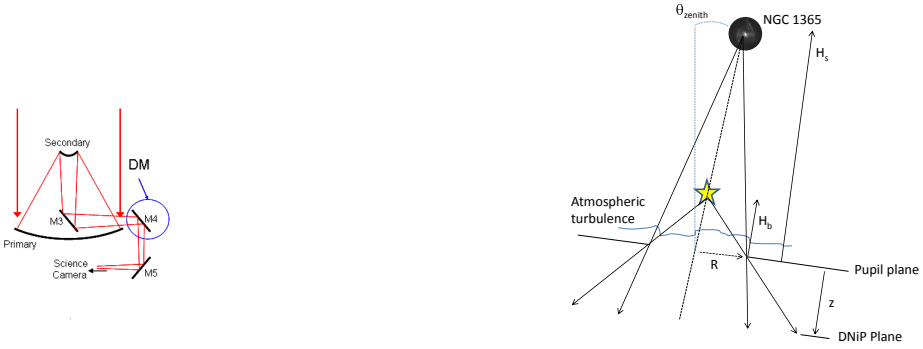

Figure 1. *DNiP geometry. Left: M4 has been replaced by a DM causing a displacement of approximately* $1Km$ *in outputspace. Right: the science object is at infinity and the sodium guidestar at approximately* $90Km$*. These two conjugates lead to the sodium beam diverging after the telescope removes the focus of the science object.*

telescope is focused on the science object, so the science beam is (stochastically) planar after the primary-secondary optical elements, (2) the DM is placed non-conjugate to the pupil, and (3) the sodium beacon is generated at approximately $90Km$ causing the sodium beacon to have a residual (de)focus after the primary-secondary optical elements. This is the geometry of one proposed design for the SOR high efficiency AO system which replaces M4 by a DM causing a displacement of approximately $1Km$ in outputspace. This is the design for which a 7-15% degradation is Strehl was noted and the design to be studied here.

3. DETERMINING THE ROOT CAUSE OF THE DEGRADATION

There are well known causes for degradation in Strehl and this degradation was initially thought by the community to be caused by focus anisoplanatism.[8]

3.1. Focus Anisoplanatism

Focus anisoplanatism arises with LGS AO because the LGS is at a finite altitude with respect to the science object (see the left plot in Figure 1). Because the beacon is at a finite altitude, it does not sample the full atmosphere experienced by the science beam. This improperly sampled atmosphere is then used as the correction for the full atmosphere causing a residual phase variance on the science beam even if the measured phase is fully corrected.

This effect is well known and has been thoroughly studied. Following Sasiela,[9] the phase variance caused by focus anisoplanatism for a spherical wave is given by

$$\sigma_{\_}^2 = 0.5k_0^2 \frac{D}{L}^{5/3} \mu_{5/3\_}, \tag{1}$$

$$\text{with } \mu_{5/3} = \int_0^L C_n^2(z)(\gamma z)^{5/3}\, dz \tag{2}$$

where D is the pupil diameter, k_0 is the wave number, L is the distance to the guide star, and C_n^2 is the atmospheric structure function, $\mu_{5/3\_}$ is the $(5/3)^{\text{th}}$ atmospheric moment, the subscript $\_$ denotes integration from the guidestar down, and the science signal is at infinity. Throughout this analysis C_n^2 is given by HV-21 (commonly known as $HV_{5/7}$), i.e.

$$C_n^2 = 0.00594 \frac{W}{27}^2 (10^{-5}h)^{10} e^{\frac{-h}{1000}} + 2.710^{-16} e^{\frac{-h}{1500}} + Ae^{\frac{-h}{100}} \tag{3}$$

where h is the altitude in meters, C_n^2 is in $m^{-2/3}$, $A = 1.710^{-14}$, and $W = 21$ a pseudo-wind term.

Note that if the disturbance is solely in the pupil then $C_n^2(h) = C_n^2(0)\delta(h)$ which implies that $\sigma^2 = 0$, which implies $S = 1$, i.e. there is no focus anisoplanatism regardless of the value of ΔL. Hence, conventional wisdom is incorrect.

But perhaps subtleties occur when C_n^2 is distributed. So, assuming a distributed atmosphere Equation 1 can be rewritten as

$$\sigma^2 = 0.5k_0^2 \frac{D}{L + \Delta L}^{5/3} \int_0^L C_n^2(z)(\frac{L + \Delta L - z}{L + \Delta L} z)^{5/3}\, dz$$

where ΔL is the distance out of the pupil. Using the standard approximation, the degradation in Strehl given by this phase variance is

$$S \sim e^{-\sigma^2} \tag{4}$$

and so the degradation caused by putting the DNiP geometry is given by $e^{-\sigma_1^2 + \sigma_2^2}$. Hence, the change in focus anisoplanatism due to the DNiP geometry causes a decrease in Strehl of 0.49% when Δ L is increased to 1 km. This is plotted in Figure 2. Hence, there is less than 1% additional degradation due to focus anisoplanatism when the DM is placed in the DNiP position for a realistic atmosphere. This conclusion is unchanged if the piston and tilt focus anisoplanatic phase variance is used. So, the degradation seen in simulation and experiment are not caused by focus anisoplanatism.

3.2. r_0, θ_0, σ_χ^2, and Greenwood frequency

There are a standard list of stochastic parameters that cause degradation in Strehl. It was thought that perhaps the degradation in Strehl was caused by changes in these parameters and this caused the degradation. So, studying how these parameters change with changes in ΔL is necessary. Specifically, this subsection modifies the expressions for r_0, Rytov, and θ_0 to account for the DM-not-in-the-pupil (DNiP) case. From physical grounds, the DNiP degradation occurs even when the science object is a star, so while the Greenwood frequency causes AO system degradation, it plays no part in the DNiP degradation and will not be discussed further.

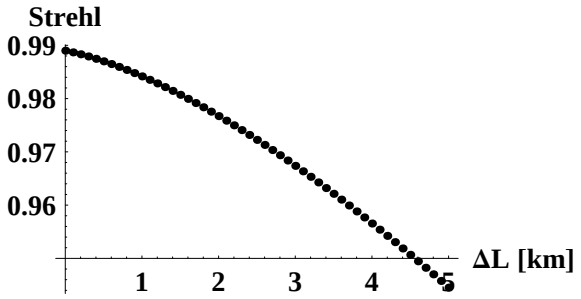

Figure 2. Degradation in Strehl caused by focus anisoplanatism as a function of ΔL

3.2.1. Fried's Parameter, Rytov, and the Isoplanatic Patch

Again following Sasiela

$$r_0 = (0.423k_0^2\mu_0)^{-3/5} = \left(0.423k_0^2\int_0^L C_n^2(z)\,dz\right)^{-3/5} \tag{5}$$

$$\sigma_\chi^2 = 0.563k_0^{7/6}\mu_{5/6} = 0.291k_0^{7/6}\int_0^L C_n^2(z)(\gamma z)^{5/6}\,dz \tag{6}$$

$$\theta_0 = 2.91k_0^2\mu_{5/3} = 2.91k_0^2\int_0^L C_n^2(z)(\gamma z)^{5/3}\,dz \tag{7}$$

with $\gamma = \frac{L-z}{L}$ for a laser guidestar geometry.

To modify the equations for the DNiP geometry with a spherical beam, L is replaced with $L+\Delta L$ and the integration is from $-\Delta L$ to L. So for a spherical beam propagating from L to 0, $\gamma = \frac{L+\Delta L-z}{L+\Delta L}$. Then, the expressions become:

$$r_0 = \left(0.423k_0^2\int_0^L C_n^2(z)\,dz\right)^{-3/5} \tag{8}$$

$$\sigma_\chi^2 = 0.291k_0^{7/6}\int_{-\Delta L}^L C_n^2(z)(\frac{L+\Delta L-z}{L+\Delta L}z)^{5/6}\,dz \tag{9}$$

$$\theta_0 = 2.91k_0^2\int_{-\Delta L}^L C_n^2(z)(\frac{L+\Delta L-z}{L+\Delta L}z)^{5/3}\,dz \tag{10}$$

But $C_n^2(z) = 0$ when $z <= 0$, so

$$r_0 = \left(0.423k_0^2\int_0^L C_n^2(z)\,dz\right)^{-3/5} \tag{11}$$

$$\sigma_\chi^2 = 0.291k_0^{7/6}\int_0^L C_n^2(z)(\frac{L+\Delta L-z}{L+\Delta L}z)^{5/6}\,dz \tag{12}$$

$$\theta_0 = 2.91k_0^2\int_0^L C_n^2(z)(\frac{L+\Delta L-z}{L+\Delta L}z)^{5/3}\,dz \tag{13}$$

Equation 11 demonstrates that r_0 does not change with ΔL. So, changes in r_0 cannot be responsible for the DNiP degradation.

Equations 12 and 13 have a form such that ΔL only appears when added to L. So for $\Delta L < L$, changes in r_0 and Rytov should be small. This is indeed the case; note as ΔL increases from 0 to 5 km, σ_χ^2 increases by 0.32%, while θ_0 decreases by 0.59 %. The 0.32% increase in scintillation corresponds to a multiplicative decrease in Strehl of $e^{-0.0032}$.

The decrease in the isoplanatic patch causes a a change in Strehl of

$$exp\left(\left(\frac{\theta}{\theta_0}\right)^2 - \left(\frac{\theta}{\theta_0 - \epsilon}\right)^2\right) \approx exp\left(\frac{2\epsilon}{\theta_0}\left(\frac{\theta}{\theta_0}\right)^2\right) < e^{-0.001} \tag{14}$$

with $\epsilon = 0.0059$ when $\Delta L = 5Km$ and the rightmost relation holding for any $\theta < \theta_0$ and $\Delta L < 5Km$. So, the DNiP degradation is not caused by changes in scintillation or the isoplanatic patch.

These results are plotted in Figures 3, 4, and 5. In each plot, the beacon is at 100 km, $\lambda = 0.5\mu m$, and the C_n^2 model used is 1x the HV-21 model.

Section Summary This section has demonstrated that the cause of the DNiP degradation is not one of the customary degradation effects. By process of elimination, the only remaining physically varying quantity is the variation in magnification between the pupil and DNiP planes. We propose that this must be the cause of the degradation. This result was reached independently by Rhoadarmer.[10] In keeping with standard notation in the AO field, we have named this degradation "magnification anisoplanatism". The next few sections work through this hypothesis.

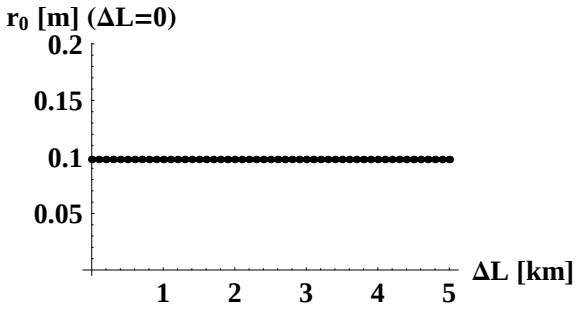

Figure 3. r_0 as a function of ΔL

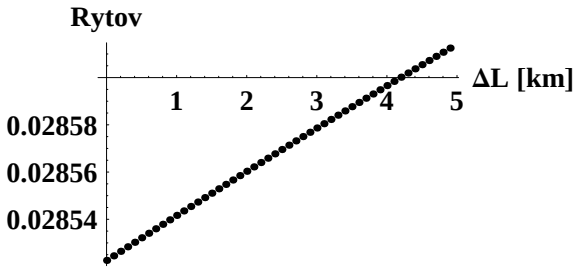

Figure 4. Scintillation as a function of Δ L

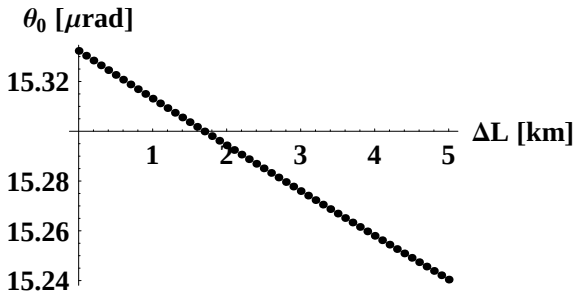

Figure 5. θ_0 as a function of ΔL

4. AN EXACT EXPRESSION VIA FRESNEL PROPAGATION

In order to gain a basic understanding of the problem, this section studies the formalism that propagates the light from the pupil plane to the DNiP plane. These propagations are well known to be Fresnel propagations.

4.1. Fresnel Propagation from the Pupil to the DNiP Plane

In general, a field at the (x,y) plane propagated from the (ξ,η) plane is described as:

$$U(x,y) = \frac{e^{ikz}}{i\lambda z}\int_{-\infty}^{\infty} d\xi \int_{-\infty}^{\infty} d\eta\, U(\xi,\eta) e^{i\frac{k}{2z}((x-\xi)^2+(y-\eta)^2)}, \tag{15}$$

where λ is the wavelength, $k = \frac{2\pi}{\lambda}$ is the wavenumber, and $U(\xi,\eta)$ is the field at the source plane. The effect of a lens is included by multiplying Equation 15 by

$$t_l(x,y) = e^{-i\frac{k}{2f}(x^2+y^2)} \tag{16}$$

where f is the focal length of the lens. In the DNiP case, the focal length of the lens at the pupil $f = z_{sci}$. So for the target, the focus error found in the phase at $e^{i\frac{k}{2z_{src}}(xi^2+\eta^2)}$ is removed with the lens term $e^{-i\frac{k}{2f}(\xi^2+\eta^2)}$ and the resulting equation for the target signal immediately after the lens is

$$U_{l-sci}(\xi,\eta) = \frac{e^{ikz_{sci}}}{i\lambda z_{sci}} \tag{17}$$

Similarly, the equation for the signal from the beacon immediately after the lens is given by

$$U_l(\xi,\eta) = e^{-i\frac{k}{2z_{sci}}(\xi^2+\eta^2)} * \frac{e^{ikz_b}}{i\lambda z_b} e^{i\frac{k}{2z_b}(\xi^2+\eta^2)} \tag{18}$$

but in this case, the focus term is not completely canceled by the lens.

$$U_l(\xi,\eta) = e^{ik(\frac{1}{2z_b}-\frac{1}{2z_{sci}})(\xi^2+\eta^2)} * \frac{e^{ikz_b}}{i\lambda z_b} \tag{19}$$

So the residual focus term is given by $e^{i\frac{k}{2}(\xi^2+\eta^2)(\frac{1}{z_b}-\frac{1}{z_{sci}})}$. The problem can be simplified further if we assume that the signal from the target and the signal from the beacon have uniform intensity at the aperture, with the added residual focus term for the signal from the beacon. This is a good approximation for astronomical imaging, where the Rytov is less than 0.1. Then, $U_{sci}(\xi,\eta) = 1$ inside the aperture with diameter D and $U_b(\xi,\eta) = e^{i\frac{k}{2}(\xi^2+\eta^2)(\frac{1}{z_b}-\frac{1}{z_{sci}})}$ inside the aperture with diameter D. These can be propagated to the DM plane

(x,y) (z_{dm} from the pupil) to determine the effect of propagating the focus error on the phase variance at the DM plane.

$$U_{sci}(x,y) = \frac{e^{ikz_{dm}}}{i\lambda z_{dm}} \int\int_{pupil} d\xi d\eta \, e^{i\frac{k}{2z_{dm}}(x-\xi)^2+(y-\eta)^2} \tag{20}$$

$$U_b(x,y) = \frac{e^{ikz_{dm}}}{i\lambda z_{dm}} \int\int_{pupil} d\xi d\eta \, e^{i\frac{k}{2z_{dm}}(x-\xi)^2+(y-\eta)^2} e^{-i\frac{k}{2}(\xi^2+\eta^2)(\frac{1}{z_b}-\frac{1}{z_{sci}})} \tag{21}$$

These two equations can be compared for various scenarios but what we really want is perfect compensation of the beacon, i.e. calculate the phase from the beacon at the DM plane and subtract this from the phase from the target signal at the DM plane. The Strehl degradation is determined by comparing the variance of the residual phase at the DM plane to the variance of the residual phase at the pupil plane. To get this expression, assume the WFS is focused at the beacon. Then, the beacon beam has no focus error. Add the propagated residual focus error (making the beam spherical again, with a source at the target) and back propagate to the pupil plane to re-create the expanding beam at the pupil. Then, remove the residual focus error to collimate the beam and forward propagate to calculate what a collimated field from the beacon would look like in the DM/WFS plane. This is done in Appendix A yielding

$$Arg\left(U(x',y')\right) = Arg\left(\frac{ik}{z'}(x'^2+y'^2)\int\int_{WFS} dxdy\, U_{meas}(x,y) e^{ik((\sqrt{\alpha}x+\frac{x'z_{sci}}{2z_{dm}^2\sqrt{\alpha}})^2+(\sqrt{\alpha}y+\frac{y'z_{sci}}{2z_{dm}^2\sqrt{\alpha}})^2)}\right) \tag{22}$$

Section Summary With this expression, we have shown that it is possible to determine the correction needed in the pupil plane based on the measured data -- the magnification hypothesis appears as scaling of the coordinates on the right hand side of the equation. However, while this is a closed form solution, it is not easily implementable on realtime AO systems.

5. PHYSICAL DESCRIPTION OF THE DEGRADATION

Assuming magnification is the cause of the degradation, it is possible to construct an expression which corrects for the degradation with an additive term; the additive term allows the correction to be implemented within existing AO control paradigms. That is, by using the gradient reference to mitigate the degradation, the DM and WFS remain both conjugate. In this manner, the DM-WFS pair remain a null seeking device with the null being a full correction of the science beam, not the beacon beam.

Notationally, $\phi(r)$ is used throughout as the science object's phase in the pupil, $\phi(ar)$ as the beacon phase measured in the DM-WFS plane, and a as the magnification. a has been calculated to be ≈ 1.06 for the proposed SOR high efficiency AO system, but for ease of calculation and in order to place an upperbound on performance $a = 1.1$ is used throughout. Also, for simplicity, the science and beacon wavelengths are assumed to be the same.

The degradation in Strehl is approximated by

$$S_{\text{DNiP}} = e^{-\sigma_\phi^2} \tag{23}$$

with σ_ϕ^2 the variance in phase caused by a non-unity magnification between the science and beacon beams. This phase variance is given by

$$\begin{aligned}
\sigma_\phi^2 &= <(\phi_{\text{science}} - \phi_{\text{beacon}})^2> - <\phi_{\text{science}} - \phi_{\text{beacon}}>^2 \\
&\quad \text{and assuming non-unity magnification} \\
&= <(\phi(r) - \phi(ar))^2> - <\phi(r) - \phi(ar)>^2 \\
&= <(\phi(r) - \phi(ar))^2> - (<\phi(r)> - <\phi(ar)>)^2 \\
&\quad \text{and because the atmosphere is a zero mean process} \\
&= <(\phi(r) - \phi(ar))^2> \\
&= <(\Delta\phi(r))^2> \\
&\quad \text{where } \Delta\phi(r) = \phi(r) - \phi(ar)
\end{aligned} \tag{24}$$

Then assuming a coarse grain derivative

$$\begin{aligned}\sigma_\phi^2 &= \delta r^2 < (\phi'(r))^2 > \\ &= \delta r^2 \ \sigma_{\phi'}^2\end{aligned} \tag{25}$$

where $\delta r = ar - r$ is assumed to be small and $\phi'(r)$ is the derivative of the phase at r.

The degradation is in Strehl due to the DNiP geometry is approximated by

$$S_{\text{DNiP}} = e^{-\delta r^2 \ \sigma_{\phi'}^2} \tag{26}$$

with $\sigma_{\phi'}^2$ the variance in the derivative of the phase.

6. MITIGATION OF THE DEGRADATION

Beginning with the results of the previous section, i.e. assuming magnification is the cause of the degradation it is trivial to write a formal solution that mitigates the degradation, i.e.

$$\phi(r) = \phi(ar) - \Delta\phi(r) \tag{27}$$

with $\phi(r)$ the science object's phase in the pupil, $\phi(ar)$ the beacon phase in the DM-WFS plane, and $\Delta\phi(r)$ an additive correction. Then, if $\Delta\phi(r)$ is added to the gradient reference, the source phase is written on the DM, the degradation is corrected, and formally the solution is in hand.

But in the real world, $\Delta\phi(r)$ is unknown. So considering astronomical imaging, i.e. $\sigma_\chi^2 < 0.2$, the phase is continuous. As such $\phi(r)$ can be expanded in a Taylor's series expansion about ar,[11] i.e.

$$\phi(r) = \sum_{k=0}^{\infty} \phi^{(k)}|_{ar} \frac{(ar-r)^k}{k!} \tag{28}$$

and

$$\phi(r) = \phi(ar) + \phi^{(1)}(ar)(ar-r) + \sum_{k=2}^{\infty} \phi^{(k)}|_{ar} \frac{(ar-r)^k}{k!} \tag{29}$$

Rearranging terms leads to

$$\begin{aligned}\Delta\phi(r) &= \phi(ar) - \phi(r) \\ &= -\phi^{(1)}(ar) \ (a-1)r - \mathcal{E}(r)\end{aligned} \tag{30}$$

with $\mathcal{E}(r) = \sum_{k=2}^{\infty} \phi^{(k)}|_r \frac{(ar-r)^k}{k!}$ the error term. Then substituting into Equation 27

$$\phi(r) = \phi(ar) + \phi^{(1)}(ar) \ (a-1)r + \mathcal{E}(r) \tag{31}$$

and dropping the error term, we obtain this section's main result

$$\phi(r) \approx \phi(ar) + \phi^{(1)}(ar) \ (a-1)r \tag{32}$$

Equation 32 is the means to correct the beacon beam phase in the DNiP plane to give a correct AO correction to the science beam in the pupil plane.

Estimation of the Error The error associated with this correction can be obtained via $\mathcal{E}(r) = \sum_{k=2}^{\infty} \phi^{(k)}|_r \frac{(ar-r)^k}{k!}$.

Since ϕ is continuus and smooth (recall $\sigma_\chi^2 < 0.2$), $b_k \to 0$ as $k \to \infty$ with b_k the k^{th} term in $\mathcal{E}(r)$, i.e. $b_k = \phi^{(k)}|_r \frac{(ar-r)^k}{k!}$. This allows us to keep a finite number of terms with confidence. In the physical system, $\phi(r)$'s maximum rate of fluctuation will be governed by Fried's parameter. In the measured and applied phase, the maximum rate of fluctuation will be governed by the DM's actuator spacing. In either case, the fluctuation fixes the maximum order of a polynomial required to fit the phase. This sets a bound on k above which the

error is negligable for any order of derivative. For instance, consider an abnormally high magnification, $a = 1.1$, then $\frac{(ar-r)^k}{k!} = \frac{(0.1r)^k}{k!}$ partially determines the rate of convergence for small k and fixes it for large k yielding for various radii the following errors

$$\begin{aligned} r = 0 \quad &\Rightarrow \left\{\frac{(0.1r)^k}{k!}\right\}_{k=2,\infty} = \{0, 0, 0, \dots\} \\ r = \tfrac{D}{4} = 0.875 \quad &\Rightarrow \left\{\frac{(0.1r)^k}{k!}\right\}_{k=2,\infty} = \{3.8 \times 10^{-3}, 1.1 \times 10^{-4}, 2.4 \times 10^{-6}, \dots\} \\ r = \tfrac{D}{2} = 1.75 \quad &\Rightarrow \left\{\frac{(0.1r)^k}{k!}\right\}_{k=2,\infty} = \{1.5 \times 10^{-2}, 8.9 \times 10^{-4}, 3.9 \times 10^{-5}, \dots\} \end{aligned} \tag{33}$$

As can be seen the error is small and has its largest values at the edge of the aperture.

In order to get a general estimate of the error, assume $\phi^{(k)} = \phi^{(j)} \quad \forall j, k \geq 2$, and we obtain

$$\mathcal{E}(r) \leq 1.5 \times 10^{-2} \ \phi^{(2)}(ar) \tag{34}$$

For $\phi^{(2)}(ar) \approx \phi^{(1)}(ar)$, the error is $\leq 1\%$, hence small but still measurable. The table below demonstrates how this technique works in the presence of a sinusiodal distrubance of amplitude π. The leftmost column is the radius of the pupil, the second column the amplitude of the phase disturbance, the third column the magnified pupil coordinates, the forth column the amplitude of the magnified phase (the beacon phase), the fifth column the correction term as given in Equation 32, the sixth column the corrected beacon phase, and the last column the error. As can be seen, for this example, the technique works as calculated.

Application of the technique to a test phase of $\pi cos(r)$. Magnification = 1.1						
radial distance (m)	science beam's phase	Correction $= \Delta\phi(r)$	magnified rad. dist. (m)	beacon beam's phase	corrected beacon phase	error
0	3.14	0	0	3.14	3.14	0.00E+000
0.25	3.04	-0.02	0.28	3.02	3.04	9.49E-004
0.5	2.76	-0.08	0.55	2.68	2.75	3.41E-003
1	1.7	-0.26	1.1	1.43	1.69	8.04E-003
1.75	-0.56	-0.54	1.93	-1.09	-0.55	1.13E-002

Wave Optics Simulation of the Correction In order to test the correction in a more realistic environment, a wave optics simulation was run. The simulation used WaveProp[12] to create recreate the DNiP sodium guidestar geometry. Typical results are plotted in Figures 6 and 7.

Figure 6 displays phase for a single frame of a single realization. The upper left plot is the phase of the science beam corrupted by the atmosphere. The beason's measured phase is displayed in the upper right plot; this is the phase that is used as the estimate of the science beam phase, i.e. it is the phase placed on the DM which corrects the science beam. The middle left plot is the correction calculated from the beacon phase to be added to the beacon phase. The middle left plot shows the beacon phase corrected via Equation 32. This corrected beacon phase is placed on the DM. The bottom plot displays a radial average of the residual error before and after correction (recall in simulation we have access to the science beam phase so it is used as truth phase). The blue curve is the uncorrected phase which shows high residual phase error, and the red curve is the corrected phase showing greatly reduced residual phase error. Note that the degradation is so small to be unobservable to the eye in the 2-D plots.

Figure 7 displays phase for a different realization. The top row is the phase of the science beam. The middle left plot is the residual phase error if this phase is corrected using beacon phase measured in the DNiP plane. The middle right plot is the residual phase error if this phase is corrected using the corrected beacon phase. The bottom row displays a radial average of the residual error before and after correction. The blue curve is the uncorrected phase which shows high residual phase error, and the red curve is the corrected phase showing greatly reduced residual phase error.

7. DISCUSSION

There remains much work to do. For instance, we don't discuss how to estimtate the derivative in the presence of beacon noise or how often should the gradient reference be updated. Also, in the dynamic case one must use the DM commands to estimate the beacon phase, i.e. use $\phi_{\text{experimental}}(ar) = \phi_{\text{DM}} + \phi_{\text{residual}}$ to calcualte $\phi^{(1)}(ar)$,

and we don't discuss implications of DM hysteresis in this estimation. Also, we don't discuss loop stability in the closed loop case (recall by adding a time varying reference to the gradient map we are effectively adding a additional small feedback loop into the closed loop AO system).

However, we did show that the degradation in performance of the proposed SOR high efficiency AO design is due to the DNiP geometry and not caused by focus anisoplanatism, r_0, θ_0, or σ_χ^2. We also demonstrated that the culprit for the DNiP degradation is magnification and given an expression to both describe the degradation and a theoretical means to mitigate the degradation.

REFERENCES

1. H. M. Martin, G. Brusa Zappellini, B. Cuerden, S. M. Miller, A. Riccardi, and B. K. Smith, "Deformable secondary mirrors for the LBT adaptive optics system," in *Advances in Adaptive Optics II. Edited by Ellerbroek, Brent L.; Bonaccini Calia, Domenico. Proceedings of the SPIE, Volume 6272, pp. 62720U (2006).*, *Presented at the Society of Photo-Optical Instrumentation Engineers (SPIE) Conference* **6272**, July 2006.
2. F. P. Wildi, G. Brusa, A. Riccardi, M. Lloyd-Hart, H. M. Martin, and L. M. Close, "Towards 1^{st} light of the 6.5m MMT adaptive optics system with deformable secondary mirror," in *Adaptive Optical System Technologies II.*, P. L. Wizinowich and D. Bonaccini, eds., *Presented at the Society of Photo-Optical Instrumentation Engineers (SPIE) Conference* **4839**, pp. 155–163, Feb. 2003.
3. G. Brusa, A. Riccardi, P. Salinari, F. P. Wildi, M. Lloyd-Hart, H. M. Martin, R. Allen, D. Fisher, D. L. Miller, R. Biasi, D. Gallieni, and F. Zocchi, "MMT adaptive secondary: performance evaluation and field testing," in *Adaptive Optical System Technologies II.*, P. L. Wizinowich and D. Bonaccini, eds., *Presented at the Society of Photo-Optical Instrumentation Engineers (SPIE) Conference* **4839**, pp. 691–702, Feb. 2003.
4. D. L. Miller, G. Brusa, M. A. Kenworthy, P. M. Hinz, and D. L. Fisher, "Status of the NGS adaptive optic system at the MMT Telescope," in *Advancements in Adaptive Optics II.*, D. Bonaccini Calia, B. L. Ellerbroek, and R. Ragazzoni, eds., *Presented at the Society of Photo-Optical Instrumentation Engineers (SPIE) Conference* **5490**, pp. 207–215, Oct. 2004.
5. R. Arsenault, R. Biasi, D. Gallieni, A. Riccardi, P. Lazzarini, N. Hubin, E. Fedrigo, R. Donaldson, S. Oberti, S. Stroebele, R. Conzelmann, and M. Duchateau, "A deformable secondary mirror for the VLT," in *Advances in Adaptive Optics II.*, *Presented at the Society of Photo-Optical Instrumentation Engineers (SPIE) Conference* **6272**, July 2006.
6. Personal communication: Dr. Barry Focoualt carried out wave optics simulations to determine the degradation in strehl for the DNiP geometry.
7. M. Mateen, D. J. Sanchez, T. Rhoadarmer, L. Arguella, D. W. Oesch, D. Fung, R. Petty, P. Kelly, R. A. Vincent, and J. Richey, "Adaptive optics with the deformable mirror not in pupil - part 1: Experimental results," in *2008 SPIE Annual Conference*, R. Carerras, T. Rhoadharmer, and J. Gonglewski, eds., Society of Professional Instrumentation Engineers, 2008. To be presented at the SPIE Annual Conference in August 2008.
8. J. M. Spinhirne, "Issues related to focal anisoplanatism in an adaptive optics system when the deformable mirror and wavefront sensor are displaced from the pupil," tech. rep., Boeing LTS, April 2007.
9. R. J. Sasiela, *Electromagnetic Wave Propagation in Turbulence: Evaluation and Application of Mellin Transforms*, SPIE Press, Bellingham, Wa, USA, 2 ed., 2007.
10. T. Rhoadarmer, "Dnip analysis," tech. rep., SAIC, March 2007. Presented in Power Point format.
11. This builds upon an idea by Jim Spinhirne.
12. T. Brennan. WaveProp is a wave optics propagation code written by Terry Brennan of tOSC.

APPENDIX A. RELATION OF THE SCIENCE BEAM TO THE BEACON BEAM

First note, the residual focus error at the pupil plane is given by $e^{\frac{ik}{2}(\xi^2+\eta^2)(\frac{1}{z_b}-\frac{1}{z_{sci}})}$. From the lens equation, $\frac{1}{z_b}+\frac{1}{f}=\frac{1}{z_{im}}$. Since $f=z_{sci}$,and z_{im} is the effective virtual image location of the expanding beam on the right side of the lens. So the residual focus error is $\frac{1}{R}=\frac{1}{z_{im}}=\frac{1}{z_b}-\frac{1}{z_{sci}}$. When the propagation is extended to the DM plane, then, the new residual focus error in the DM/WFS plane is $e^{\frac{ik}{2}(x^2+y^2)(\frac{1}{R'})}$, where $R'=R+z_{dm}$, so $\frac{1}{R'}=\frac{1}{R+z_{dm}}$.

Suppose there is some field $U_{meas}(x,y)$ at the DM/WFS plane, measured by the WFS focused at the beacon. This is the field measured by the WFS, and there should be no residual focus error on it. We are going to use this field to re-create the field from the beacon seen by the DM. When the residual focus error at the DM/WFS plane is added, the field becomes:

$$U(x,y) = U_{meas}(x,y)e^{\frac{ik}{2}(x^2+y^2)\frac{1}{R'}} \tag{35}$$

Back propagate this to the pupil plane. (For back propagation, k = -k).

$$U_{back}(\xi,\eta) = \frac{e^{-ikz_{dm}}}{i\lambda z_{dm}} \int\int_{WFS} dxdy\, U_{meas}(x,y)e^{\frac{ik}{2}(x^2+y^2)\frac{1}{R'}} e^{i\frac{-k}{2z_{dm}}((x-\xi)^2+(y-\eta)^2)} \tag{36}$$

Now, remove the residual focus error at the pupil plane (effectively, send it through the lens with $f = z_{sci}$). Then,

$$U(\xi,\eta) = e^{\frac{-ik}{2z_{sci}}(\xi^2+\eta^2)}U_{back}(\xi,\eta) \tag{37}$$

Finally, propagate back to the WFS/DM plane and compare to the original $U_{meas(x,y)}$.

$$U(x',y') = \frac{e^{ikz_{dm}}}{i\lambda z_{dm}} \int\int_{pup} d\xi d\eta\, e^{\frac{ik}{2z_{dm}}((\xi-x')^2+(\eta-y')^2)}U(\xi,\eta) \tag{38}$$

Now, simplify this equation to obtain a relationship between $U(x',y')$ and $U_{meas}(x,y)$. The equation for U(x',y') with all terms included is shown below

$$\begin{aligned} U(x',y') =& \frac{e^{ikz_{dm}}}{i\lambda z_{dm}} \int\int_{pup} d\xi d\eta\, e^{\frac{ik}{2z_{dm}}((\xi-x')^2+(\eta-y')^2)} e^{\frac{-ik}{2z_{sci}}(\xi^2+\eta^2)} \frac{e^{-ikz_{dm}}}{i\lambda z_{dm}} * \\ & \int\int_{WFS} dxdy\, U_{meas}(x,y)e^{\frac{ik}{2}(x^2+y^2)\frac{1}{R'}} e^{i\frac{-k}{2z_{dm}}((x-\xi)^2+(y-\eta)^2)} \end{aligned}$$

For now, we can work with the 1D case $U(x')$. (The 2D case has y, η and y' added in the exponents to y, ξ, and x', respectively, so it is trivial to extend to the 2D case after simplifying the equation).

$$U(x') = \frac{e^{ikz_{dm}}}{i\lambda z_{dm}} \int_{pup} d\xi\, e^{\frac{ik}{2z_{dm}}(\xi-x')^2} e^{\frac{-ik}{2z_{sci}}\xi^2} \frac{e^{-ikz_{dm}}}{i\lambda z_{dm}} \int_{WFS} dx\, U_{meas}(x)e^{\frac{ik}{2}x^2\frac{1}{R'}} e^{i\frac{-k}{2z_{dm}}(x-\xi)^2} \tag{39}$$

To simplify this, put everything inside all of the integrals and expand the quadratics in the exponents. Group terms with like x, y, x', y', ξ, η, and take x' and y' terms out of the integrals. Then switch the order of integration, which is possible because the fields are smooth and finite.

$$U(x') = \frac{1}{-(\lambda z_{dm})^2} \int_{pup} d\xi \int_{WFS} dx\, U_{meas}(x)e^{\frac{-ik}{z_{dm}}(x'\xi)} e^{\frac{ik}{2z_{dm}}(x'^2)} e^{\frac{-ik}{2z_{sci}}(\xi^2)} e^{\frac{ik}{2}(x^2)\frac{1}{R'}} e^{\frac{ik}{z_{dm}}(x\xi)} e^{\frac{-ik}{2z_{dm}}(x^2)} \tag{40}$$

$$U(x') = \frac{1}{-(\lambda z_{dm})^2} e^{\frac{ik}{2z_{dm}}x'^2} \int_{WFS} dx\, U_{meas}(x)e^{ikx^2(\frac{1}{R'}-\frac{1}{2z_{dm}})} \int_{pup} d\xi\, e^{-ik(\xi^2\frac{1}{2z_{sci}}-\xi\frac{(x-x')}{z_{dm}})} \tag{41}$$

Look at the inner integral, over the pupil. By completing the square, $ax^2+bx+c = (\sqrt{a}x+\sqrt{c})^2$. Then $b = 2\sqrt{ac}$. So

$$\xi^2\frac{1}{2z_{sci}} + \xi\frac{(x-x')}{z_{dm}} = (\frac{1}{\sqrt{2z_{sci}}}\xi + \frac{(x-x')}{z_{dm}}\sqrt{\frac{z_{sci}}{2}})^2 - \frac{(x-x')^2}{z_{dm}^2}\frac{z_{sci}}{2} \tag{42}$$

Let $u = \frac{1}{\sqrt{2z_{sci}}}\xi + \frac{(x-x')}{z_{dm}}\sqrt{\frac{z_{sci}}{2}}$. Then the integral is

$$\sqrt{2z_{sci}}e^{ik\frac{(x-x')^2 z_{sci}}{2z_{dm}^2}} \int_{pup} du\, e^{-iku^2} \tag{43}$$

This integral is known to be $-\frac{(-1)^{1/4}\sqrt{\pi}Erf(i(-1)^{3/4}\sqrt{k}u)}{i2\sqrt{k}}$, and recall that $(-1) = e^{i\pi}$

$$\sqrt{2z_{sci}}e^{ik\frac{(x-x')^2 z_{sci}}{2z_{dm}^2}}[-\frac{\sqrt{\pi}Erf(\sqrt{k}u)}{2\sqrt{k}}]_{u=-\infty}^{u=\infty} \tag{44}$$

The error function gives 1 and ∞ and -1 at $-\infty$, so

$$\sqrt{2z_{sci}}e^{ik\frac{(x-x')^2 z_{sci}}{2z_{dm}^2}}[-\frac{\sqrt{\pi}}{2\sqrt{k}} - \frac{\sqrt{\pi}}{2\sqrt{k}}] = -\sqrt{\frac{2\pi z_{sci}}{k}}e^{ik\frac{(x-x')^2 z_{sci}}{2z_{dm}^2}} \tag{45}$$

Throw this back into the equation for the field at (x', y'), and you have:

$$U(x') = \frac{\sqrt{2\pi z_{sci}}}{\sqrt{k}(\lambda z_{dm})^2}e^{\frac{ik}{2z_{dm}}x'^2}\int_{WFS} dx\, U_{meas}(x)e^{ikx^2(\frac{1}{R'}-\frac{1}{2z_{dm}})}e^{ik\frac{(x-x')^2 z_{sci}}{2z_{dm}^2}} \tag{46}$$

Expand the quadratics again and simplify:

$$U(x') = \frac{\sqrt{2\pi z_{sci}}}{\sqrt{k}(\lambda z_{dm})^2}e^{\frac{ik}{2z_{dm}}x'^2}\int_{WFS} dx\, U_{meas}(x)e^{ikx^2(\frac{1}{R'}-\frac{1}{2z_{dm}})}e^{ik\frac{z_{sci}}{2z_{dm}^2}(x^2-2x'x+x'^2)} \tag{47}$$

$$U(x') = \frac{\sqrt{2\pi z_{sci}}}{\sqrt{k}(\lambda z_{dm})^2}e^{ikx'^2(\frac{1}{2z_{dm}}+\frac{z_{sci}}{2z_{dm}^2})}\int_{WFS} dx\, U_{meas}(x)e^{ik(x^2(\frac{1}{R'}-\frac{1}{2z_{dm}}+\frac{z_{sci}}{2z_{dm}^2})-x(\frac{z_{sci}}{z_{dm}^2}x')} \tag{48}$$

Let $\alpha = \frac{1}{R'} - \frac{1}{z_{dm}} + \frac{z_{sci}}{z_{dm}^2}$. Complete the square again, with $a = \sqrt{\alpha}, b = \frac{x' z_{sci}}{z_{dm}^2}, c = \frac{x'^2 z_{sci}^2}{4\alpha z_{dm}^4}$. Then

$$U(x') = \frac{\sqrt{2\pi z_{sci}}}{\sqrt{k}(\lambda z_{dm})^2}e^{ikx'^2(\frac{1}{2z_{dm}}+\frac{z_{sci}}{2z_{dm}^2}-\frac{z_{sci}^2}{4\alpha z_{dm}^4})}\int_{WFS} dx\, U_{meas}(x)e^{ik(\sqrt{\alpha}x+\frac{x' z_{sci}}{2z_{dm}^2\sqrt{\alpha}})^2} \tag{49}$$

This can't be analyzed further without $U_{meas}(x)$. Let $\frac{1}{z'} = \frac{1}{2z_{dm}} + \frac{z_{sci}}{2z_{dm}^2} - \frac{z_{sci}^2}{4\alpha z_{dm}^4}$. Then the 2D version looks like this:

$$U(x', y') = \frac{\sqrt{2\pi z_{sci}}}{\sqrt{k}(\lambda z_{dm})^2}e^{\frac{ik}{z'}(x'^2+y'^2)}\int\int_{WFS} dxdy\, U_{meas}(x, y)e^{ik((\sqrt{\alpha}x+\frac{x' z_{sci}}{2z_{dm}^2\sqrt{\alpha}})^2+(\sqrt{\alpha}y+\frac{y' z_{sci}}{2z_{dm}^2\sqrt{\alpha}})^2)} \tag{50}$$

Any possibile mitigation of the degradation only considers phase, so

$$Arg\left(U(x', y')\right) = Arg\left(\frac{ik}{z'}(x'^2 + y'^2)\int\int_{WFS} dxdy\, U_{meas}(x, y)e^{ik((\sqrt{\alpha}x+\frac{x' z_{sci}}{2z_{dm}^2\sqrt{\alpha}})^2+(\sqrt{\alpha}y+\frac{y' z_{sci}}{2z_{dm}^2\sqrt{\alpha}})^2)}\right) \tag{51}$$

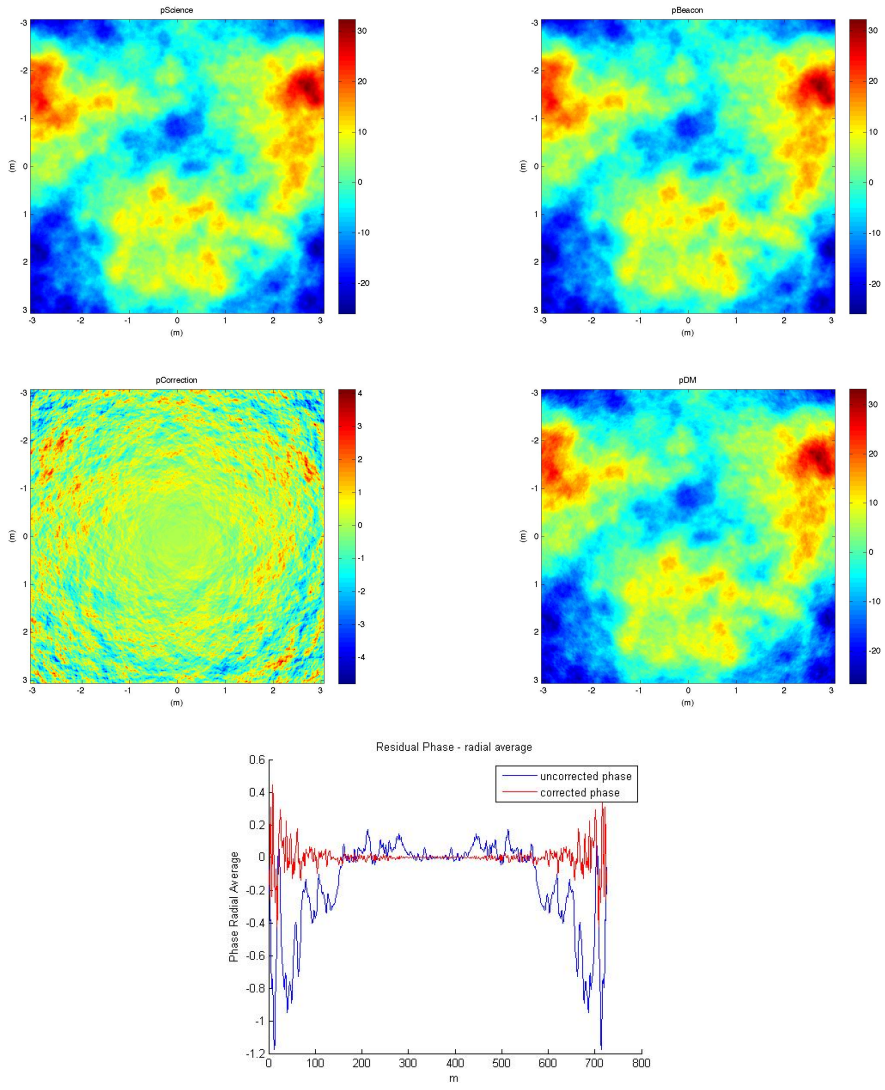

Figure 6. Top row: science beam phase (left) and beacon beam phase (right). Middle row: correction phase (left) and corrected beacon phase (right). Bottom row: radial average of residual phase error, blue: uncorrected phase showing high residual phase error, red: corrected phase showing greatly reduced residual error. As can be seen the degradation and the correction terms are small but measureable.

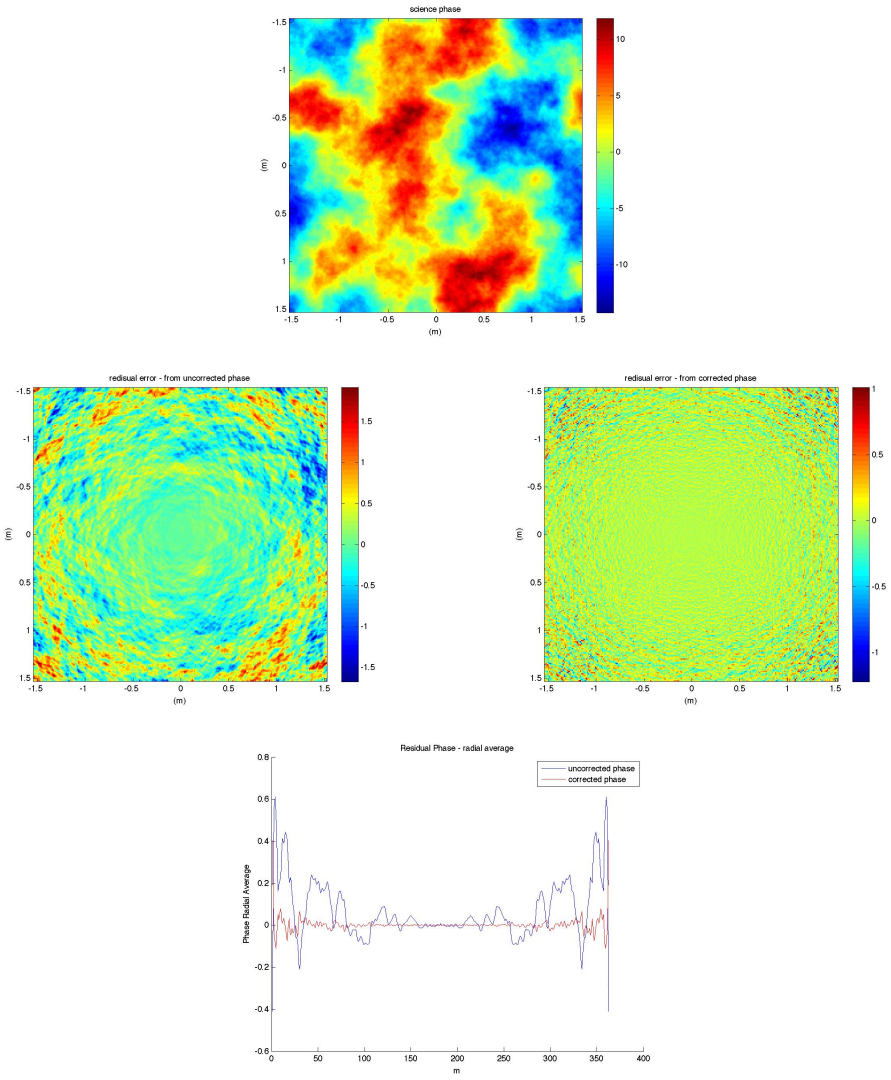

Figure 7. Top row: science beam phase. Middle row: residual phase error uncorrected (left) and corrected residual phaser error (right). Bottom row: radial average of residual phase error, blue: uncorrected phase showing high residual phase error, red: corrected phase showing greatly reduced residual error. As can be seen the degradation and the correction terms are small but measureable.

DISTRIBUTION LIST

DTIC/OCP
8725 John J. Kingman Rd, Suite 0944
Ft Belvoir, VA 22060-6218 1 cy

AFRL/RVIL
Kirtland AFB, NM 87117-5776 2 cy

Pat Kelly
Official Record Copy
AFRL/RDSA 1 cy